Estuarine, Coastal and Shelf Science 270 (2022) 107831

Contents lists available at ScienceDirect

Estuarine, Coastal and Shelf Science

journal homepage: www.elsevier.com/locate/ecss

Land-cover, climate and fjord morphology drive differences in organic matter and nutrient dynamics in two contrasting northern river-fjord systems

Sabrina Schultze [a,**], Tom Andersen [a], Dag O. Hessen [a], Anders Ruus [a,b], Katrine Borgå [a], Amanda E. Poste [b,c,*]

[a] University of Oslo, Department of Biosciences, Aquatic Biology and Toxicology and Centre for Biogeochemistry in the Anthropocene, 0316, Oslo, Norway
[b] Norwegian Institute for Water Research, Økernveien 94, 0579, Oslo, Norway
[c] UiT–The Arctic University of Norway, 9037, Tromsø, Norway

A R T I C L E I N F O

Keywords:
Coastal darkening
Estuary
Organic matter
Seasonality
Climate change
Biogeochemistry
Land-ocean interactions

A B S T R A C T

Climate and land-use changes are leading to impacts on individual ecosystems as well as shifts in transfer dynamics between interconnected systems. At the land-ocean interface, changes in riverine inputs of organic matter (OM) and nutrients have the potential to lead to shifts in coastal carbon and nutrient cycling with consequences for ecosystem structure and function. In this study, we assess OM and nutrient dynamics for two contrasting Norwegian river-to-fjord systems: a boreal system with a forested catchment draining into a narrow fjord ('narrow boreal system'), and a subarctic system where lowland forests and mountainous regions drain into a broad fjord ('broad subarctic system'). We characterized seasonal organic carbon and nutrient concentrations and DOM absorption properties for samples collected along transects from river to outer fjord during 2015/2016. While differences in catchment properties drove contrasts in river chemistry between the two study rivers, fjord morphology and hydrodynamics as well as dissolved organic carbon (DOC) and nutrient concentrations in marine receiving waters predicted water-chemistry patterns along the transect. The narrow boreal system, with high riverine DOC and nutrient concentrations, was structured mainly by a horizontal salinity gradient from river to outer fjord, with limited impact of seasonality. In contrast, the broad subarctic system tended to be dominated by vertical salinity stratification, with strong between-date differences in surface water salinity linked to seasonality in river discharge. These dynamics were also reflected in the strong horizontal gradients in DOC, nutrients and DOM properties in the narrow boreal system, in contrast to the broad subarctic system, where strong seasonality paired with a lack of strong contrast between riverine and marine concentrations of DOC and most nutrients led to an uncoupling between salinity and other water chemistry variables. In the narrow boreal system, terrestrial OM dominated both the particulate and dissolved OM pools, while OM in the broad subarctic system was derived primarily from marine phytoplankton. Non-linear declines in $NO_3 + NO_2$ were observed consistently in the boreal system and during the productive spring season in the subarctic system, suggesting biological uptake and a potentially important role of these rivers as sources of bioavailable N to coastal ecosystems. The results from these two case studies highlight the complex and interacting effects of catchment land-cover, river water chemistry and discharge, fjord morphometry and hydrodynamics in structuring the transport, fate and potential impacts of terrestrially-derived nutrients and organic matter in northern coastal environments.

1. Introduction

River systems link the land to the sea by transporting compounds of terrestrial origin, such as organic matter, nutrients, sediments as well as anthropogenic contaminants (Kominoski et al., 2020; McGovern et al., 2019; Ripszam et al., 2015; Tolkkinen et al., 2020). Estuarine systems are of particularly high ecological and economic importance as providers of essential ecosystem services such as disturbance regulation,

* Corresponding author. Norwegian Institute for Water Research, Økernveien 94, 0579, Oslo, Norway.
** Corresponding author.
E-mail addresses: sabrina.schultze@ibv.uio.no, sabrina.schultze@niva.no (S. Schultze), amanda.poste@niva.no (A.E. Poste).

https://doi.org/10.1016/j.ecss.2022.107831
Received 9 April 2021; Received in revised form 26 February 2022; Accepted 28 March 2022
Available online 31 March 2022

nutrient cycling, diversity hotspots, fish nurseries and recreational areas (Colombano et al., 2020; Costanza et al., 1997; Nagelkerken et al., 2015). In many temperate and high latitude regions, fjords represent a common type of estuarine system, where riverine (or glacial) inputs paired with geomorphological characteristics create strong physical, chemical and ecological gradients, and where carbon burial rates can be very high (Bianchi et al., 2020). These features, paired with the likely sensitivity of fjord ecosystems to several climate and other human stressors, have led to the classification of fjords as 'Aquatic Critical Zones' that require detailed study (Bianchi et al., 2020).

The degree of connectivity in an estuarine system (i.e. the "water mediated transfer of matter, energy, and/or organisms within or between elements of the hydrological cycle", as defined by (Pringle, 2001) determines the origin and thus quantity and quality of nutrients and organic matter (OM) available to organisms at any given time, thus directly impacting productivity and food web structure in these transition zones (Turner et al., 1998). Meanwhile, the residence time of freshwater in an estuary, which is linked to freshwater discharge into the system and estuarine hydrodynamics (including stratification) also plays a key role in shaping the processing and fate of terrestrially derived nutrients and OM in estuarine, including fjord environments (Bianchi et al., 2020).

In recent years, an increase in terrestrial dissolved organic matter (DOM_{terr}) has been observed in many northern freshwater, coastal and marine systems (Creed et al., 2018; de Wit et al., 2021; Dupont and Aksnes, 2013; McGovern et al., 2019; Opdal et al., 2019). This phenomenon is commonly referred to as "browning" in lakes and rivers, and "darkening" in coastal areas, and has become a major concern (Creed et al., 2018; de Wit et al., 2016; Jonsson et al., 2017). Dissolved organic matter (DOM) is operationally defined as OM that passes through a filter with a given pore size (typically between 0.2 and 0.7 μm (Xu and Guo, 2017). Browning and darkening are linked to the conspicuous brown colour of terrestrially derived (allochthonous) DOM, related to the absorption properties of high molecular weight humic and fulvic acids with aromatic components. In comparison, DOM produced by aquatic autotrophs (autochthonous; hereafter referred to as DOM_{mar}) is mainly composed of lower molecular weight aliphatic constituents (Chiou et al., 1986; Ripszam et al., 2015). Mobilization and delivery of DOM_{terr} (and nutrients) to downstream waterbodies is impacted by several catchment processes including acid rain deposition, land use, terrestrial primary production, temperature and precipitation/runoff (de Wit et al., 2021; Evans et al., 2005; Finstad et al., 2016; Larsen et al., 2011) as well as bacterial and fungal activity (Tolkkinen et al., 2020).

Depending on climate, catchment properties and landuse, terrestrial runoff can have widely different impacts on ecosystem stability and productivity of estuarine and subsequently adjacent marine systems (Creed et al., 2018; Jonsson et al., 2017; Leroux and Loreau, 2008; Lønborg et al., 2020). While inputs from land are important sources of inorganic nutrients to aquatic primary producers (Paczkowska et al., 2020; Terhaar et al., 2021), increased input of DOM_{terr} can either positively or negatively affect primary production (Thrane et al., 2014). DOM_{terr} may serve as a major source of organic nutrients (mainly dissolved organic nitrogen, dissolved organic phosphorus and iron) and thus can be important to primary and secondary production (Creed et al., 2018 and reference therein). However, at higher loads of DOM_{terr}, increased DOM-associated light-attenuation may override these potential positive impacts (Creed et al., 2018; Thrane et al., 2014). Inputs of DOM_{terr} can affect the prevalence of heterotrophic bacteria (Creed et al., 2018; Hessen et al., 1990; Sipler et al., 2017), the activities of organisms that rely on visible cues (Bartels et al., 2016; Estlander et al., 2010) as well as contaminant cycling and bioavailability (Arnold et al., 2009; Chiou et al., 1986; Cooper and Zika, 1983; McGovern et al., 2019; Mostofa and Sakugawa, 2009; Wolf et al., 2018).

The potential effects of mobilization and transport of DOM_{terr} and terrestrial nutrients to downstream freshwater and coastal ecosystems depend on transformation, uptake and removal processes along the aquatic continuum, which shape nutrient and OC concentrations as well as DOM quality from headwater to coast (Kothawala et al., 2021; Massicotte et al., 2017). Thus understanding DOM sources, patterns and effects in estuary systems depends on investigating the interconnectivity between multiple ecosystem compartments such as terrestrial-riverine and riverine-marine systems (Kothawala et al., 2021).

The character of DOM_{terr} depends strongly on catchment properties (e.g. Asmala et al., 2013) and changes along the freshwater-marine continuum as it is degraded by sunlight and bacteria (Cory et al., 2014; Fabian et al., 2017; Koehler et al., 2014). Along this continuum, there is also often an increasing contribution of marine phytoplankton derived DOM_{mar} to the total DOM pool (Ye et al., 2018), as also observed in the current study. DOM derived from phytoplankton is typically more readily taken up and transformed by coastal microbial communities than DOM_{terr} (Creed et al., 2018), with DOM uptake (regardless of origin) also dependent on nutrient availability (Asmala et al., 2018). Strong seasonality and spatial variability (e.g. horizontal and vertical 'patchiness') in primary production in northern coastal ecosystems will also be reflected in DOM character, with local-to regional-scale and short term impacts of algal bloom events (Danhiez et al., 2017). Flocculation of DOM due to e.g. changes in water chemistry (and especially increased salinity) is likely to reduce overall DOM transmission along the estuarine gradient (especially for Fe-rich DOM), and may deliver a substantial fraction of riverine OM (and OM-associated nutrients) to the sediments, limiting export to the open sea and representing an important carbon sink (Asmala et al., 2014; Hessen et al., 2010).

These changes in source and character of DOM are often inferred based on changes in absorption properties of DOM, using metrics derived from measured absorption spectra that are known to be correlated with specific DOM sources and properties. For example, specific UV absorbance at 254 nm ($SUVA_{254}$) use used as an indicator of high aromaticity of DOM; (Weishaar et al., 2003); the ratio of absorption at 250 nm–365 nm (E2:E3) can indicate low molecular weight and aromaticity (De Haan and De Boer, 1987; Peuravuori and Pihlaja, 1997); and the spectral slope between 275 and 295 nm (S275:S295) indicates lower molecular weight DOM, including photochemically-degraded DOM (Helms et al., 2008; Twardowski et al., 2004). $\delta^{13}C$ values can also be used to indicate the source of dissolved or particulate organic carbon in a system with terrestrial organic carbon tending to have lower $\delta^{13}C$ values (approximately -26‰) than OM derived from marine primary producers (around -23‰; but can be highly variable) (Peterson and Fry, 1987).

Estuarine geomorphology is of major importance in determining the physical, biogeochemical and ecological impacts of riverine inputs on estuaries (including fjords). Connectivity to the open ocean and tidal range can, for example, affect marine water intrusion and mixing patterns (Bianchi et al., 2020). Meanwhile, longer estuarine/fjord freshwater residence times can allow for e.g. higher losses to the sediments, photochemical and/or microbial mineralization of DOM, and biological uptake in the coastal environment (as reviewed in Bianchi et al., 2020).

Nutrient inputs may support both autotrophic and heterotrophic production along the freshwater-marine continuum depending on the predominant limitation processes, and in particular on spatial patterns and seasonal changes in light attenuation, nutrient concentrations, as well as organic matter availability and composition. In high latitude areas with strong seasonality in discharge and in catchments that are small, and/or have limited hydrologic connectivity, terrestrial runoff often enters streams, rivers, and downstream coastal ecosystems as intense 'pulses' linked to snowmelt and rainfall events (Avagyan et al., 2016; Köhler et al., 2008; Raymond et al., 2016), while in larger systems and/or systems that experience less seasonality in discharge (or low frequency of flood events), there will be lower intra-annual variability in riverine inputs to the coastal environment. These system-specific seasonal differences, paired with seasonality in key physical, biogeochemical and ecological processes in the coastal environment (e.g. timing of phytoplankton blooms or periods of nutrient limitation, seasonality in stratification/mixing) will affect the distribution and fate of riverine OM and nutrients, and ultimately the organisms living downstream (Bianchi et al., 2020; Frigstad et al., 2020; Opdal et al., 2019).

The aim of the present study was to characterize and contrast OM and nutrient dynamics in two Norwegian river-to-fjord 'case study' systems, focusing on changes in OM and water chemistry along the river-to-fjord continuum as well as the role of seasonality in shaping the observed patterns. The selected case study systems differ in their climate, catchment properties, river water chemistry as well as their fjord morphology, providing an opportunity to identify more general as well as fjord specific drivers of OM and nutrient cycling.

2. Material and methods

2.1. Study sites

The study sites included two contrasting Norwegian river-to-fjord systems: 1) the Storelva-Sandnesfjord system (hereafter: narrow boreal system) in southern Norway, characterized by a boreal climate, high riverine nutrient and organic carbon concentrations, a narrow opening towards the ocean and a relatively restricted tidal range; and 2) the Målselv-Målselvfjord system (hereafter: broad subarctic system) in Northern Norway, characterized by lower riverine nitrogen and organic carbon concentrations, an open connection to the ocean, strong seasonality in river discharge and a stronger tidal influence than the narrow boreal system.

The narrow boreal system (located at 58°40′13.0″N, 8°58′51.5″E, Fig. 1) has a catchment area of 408 km^2 dominated by forests and is sparsely populated, but also includes some areas with past mining activity. There are roads with heavy traffic along some parts of the river, which is also limed to stabilize the pH in this catchment where recovery from acidification is ongoing. Median river discharge from 2011 to 2016 was 6.88 m^3/s (at the Lundevann hydrologic monitoring station operated by the Norwegian watercourse and energy directorate (NVE), data from http://sildre.nve.no/, accessed 01.2021). The river discharges into a deep basin in the inner fjord where brackish waters are trapped by a shallow sill, leading to strong stratification and a permanently anoxic brackish deep water layer (Fig. 2a). Station B, the second station downstream, is located in this deep basin. The tidal monitoring station near the narrow boreal system had a yearly average water level of 53 cm and 48 cm above chart datum with minimum and maximum tides of −16 cm and −16 cm, and 155 cm and 157 cm, in 2015 and 2016 respectively (measured at Helgeroa - 58°59′37.4″N, 9°51′30.2″E; (Kartverket, 2020)). The breadth of the estuary at respective sampling sites varies between approx. 10 m (River) and 1043 m (Station F; station G is marine and not directly surrounded by land) (Table S1).

The broad northern system Målselv-Målselvfjord (hereafter: broad subarctic system) is located in sub-arctic northern Norway (69°19′39.0″N, 18°30′54.4″E, Fig. 1). The catchment area of 5913 km^2 is dominated by mountain areas and forests, and is largely undisturbed (Skarbøvik et al., 2013). The median river discharge from 2011 to 2016 was 48.03 m^3/s (measured at the Målselvfossen hydrologic monitoring station operated by NVE; data from http://sildre.nve.no/', accessed 01.2021). The inner fjord is characterized by an extensive shallow delta (where our innermost station is located) that drops off rapidly to more than 100 m towards the outer fjord (Fig. 2b). The measurement station closest to the broad subarctic system had a yearly average water level of 143 cm and 135 cm above chart datum with a minimum and maximum tide level of −21 cm and −20 cm, and 307 cm and 292 cm, in 2015 and 2016 respectively (measured at Harstad 68°47′40.7″N, 16°32′49.7″E (Kartverket, 2020)). The breadth of the estuary at the respective sampling sites ranges from approx. 140 m at the innermost fjord station and 7040 m in the outer fjord (Table S1).

2.2. Field sampling

Fieldwork was conducted at both estuaries once in 2015 and on several occasions in 2016 to provide data from a range of seasonal conditions (Table 1). The narrow boreal transect included 6 stations (Fig. 1) from river to outer fjord while the broad subarctic system included 5 stations (Fig. 1) from river to outer fjord. In the narrow boreal system, an additional station located further offshore (station G) was included in 2016 to capture more 'truly' marine conditions, while one intermediate station was dropped (station E). In the narrow boreal system, discharge was relatively stable across seasons, while pronounced seasonal differences occurred in the broad subarctic system (Fig. S1).

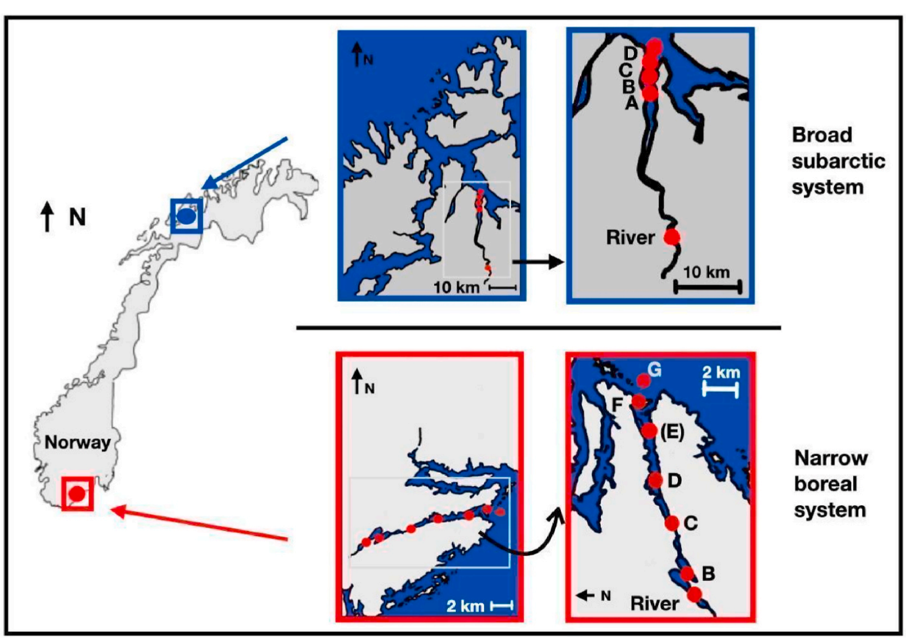

Fig. 1. Map of the broad subarctic (Målselv-Målselvfjord) and the narrow boreal (Storelva-Sandnesfjord) study systems and sampling transects. Coordinates for sampling stations are available in Table S1 in the appendix. Illustrations based on Google maps (2021).

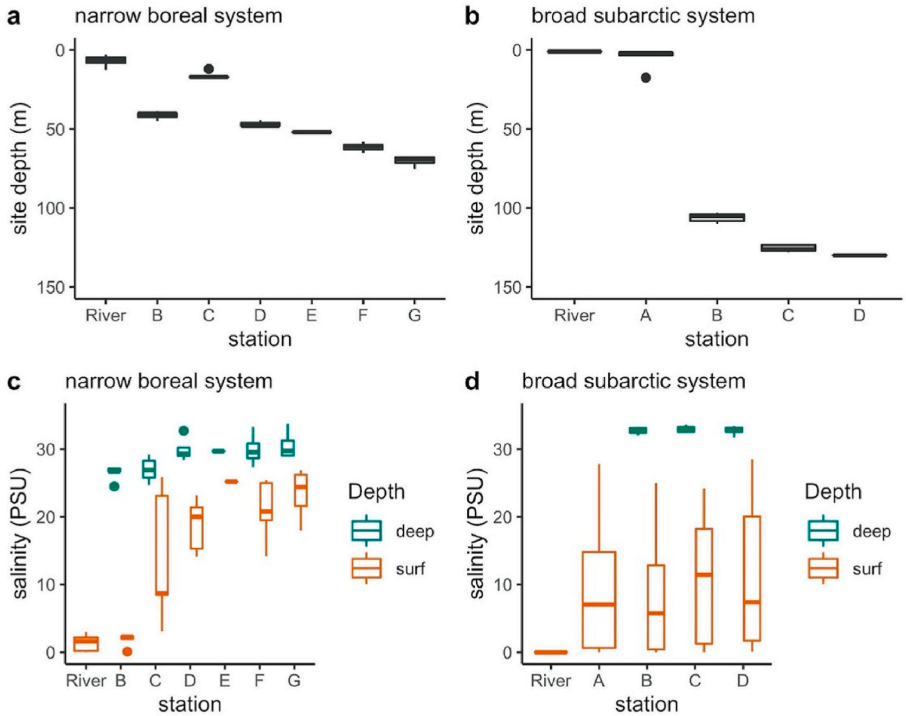

Fig. 2. Depth profiles (a; b) and salinity values (c, d) for the narrow boreal and the broad subarctic system. The depth data include measurements on all sampling dates with variability representing slight differences in exact sampling location. Salinity data are shown from both sampling depths (blue: surface, red: deep). (For interpretation of the references to colour in this figure legend, the reader is referred to the Web version of this article.)

Table 1
Sampling dates and times, mean river discharge (see also Fig. S1) for the sampling date and for the 10 days prior to sampling, and tidal levels during fjord sampling for the two study systems.

Sampling date	Sampling time	Mean discharge on sampling date[a] (m^3/s)	10-day mean discharge[a] (m^3/s)	Maximum water level during fjord sampling[b] (cm above chart datum)	Minimum water level during fjord sampling[b] (cm above chart datum)
Narrow boreal system					
May 18, 2015	10:50–18:10	5.64	9.03	57	26
April 06, 2016	11:20–17:00	21.50	26.53	72	43
May 26, 2016	11:50–16:50	6.25	5.43	35	21
August 30, 2016	11:10–17:10	9.11	10.31	71	42
October 27, 2016	11:20–17:00	10.81	12.92	74	55
Broad subarctic system					
August 26, 2015	10:00–16:30	127.92	145.21	183	75
March 14, 2016	10:40–13:00	34.09	33.25	102	32
April 19, 2016	10:40–13:30	30.98	33.29	202	178
June 01, 2016	10 a.m. at river; 15:00–17:20 other stations	628.53	440.65	40	15
August 14, 2016	13:30–16:00, River sampled August 15, 2016	189.00	211.80	130	69
November 02, 2016	10:50–13:00	59.66	62.71	128	209

[a] Discharge data for both rivers are from the Norwegian watercourse and energy directorate (NVE), with data for Storelva taken from the Lundevann hydrologic monitoring station, ~500 m upstream of our river sampling station (accessed 08.2017 at http://sildre.nve.no/), and data for Målselv taken from the Målselvfossen hydrologic monitoring station, ~20 km upstream of our river sampling station (accessed 07.2018 at http://sildre.nve.no/). Note that a large tributary joins the Målselv river between the hydrologic monitoring station and our sampling station (and the fjord), and total discharge from the river to the fjord was estimated by upscaling the discharge at Målselvfossen (catchment area: 3239 km^2) to the entire catchment area (5913 km^2).
[b] Data on tidal level are from the Norwegian Mapping Authority (Kartverket; accessed at http://www.sjokart.no).

Water was collected from just below surface and at 20 m depth, with the exception of the river stations (only surface water collected) and two stations that were too shallow: This includes station A in the broad subarctic system (no deep-water sample collected), and station C in the narrow boreal system (deep water samples taken from 8 to 10 m depth). Samples were kept cool and dark during transport to the laboratory, where they were processed immediately. Samples from the narrow boreal system were processed at the Norwegian Institute for Water Research (NIVA) in Oslo, while samples from the broad subarctic system were processed at UiT–The Arctic University of Norway (Tromsø, Norway).

Subsamples of whole water were transferred to HDPE bottles for analysis of pH and salinity (measured using the Practical Salinity Scale) and remained unpreserved until analysis. Meanwhile, subsamples of whole water for analysis of total organic carbon (TOC), total Nitrogen (N) and Phosphorus (P) were transferred to separate bottles (acid-washed brown amber glass bottles for TOC, and acid-washed HDPE bottles for total N and P) and preserved with concentrated H_2SO_4 (1% by volume). Samples for analysis of DOC and dissolved inorganic nutrients were filtered through a 0.2 μm polycarbonate filter and transferred to separate bottles (amber glass for DOC and HDPE for dissolved nutrients) and preserved as described for TOC and total N and P. Samples for optical characterization of DOM were also filtered through a 0.2 μm polycarbonate filter, but were kept unpreserved in 15 mL Falcon tubes. All water samples were kept in the cold and dark until analysis.

Samples for analysis of chlorophyll *a* (Chl a) were collected on non-combusted Whatman GF/F filters (nominal pore size of 0.7 μm), while samples for analysis of suspended particulate matter (SPM) were collected on pre-combusted and pre-weighed GF/F filters. Samples for stable carbon isotope analysis ($\delta^{13}C$) of POM were collected on pre-combusted GF/F filters. All filters were kept frozen until analysis.

2.3. Sample analysis

Water samples for organic carbon and nutrient analyses were analysed at NIVA using standard and accredited methods (Kaste et al., 2018). Chlorophyll *a* (and pheophytin) was determined fluorometrically at UiT–The Arctic University of Norway (Norway). Briefly, filters were methanol extracted and fluorescence was measured on a Turner 10-AU fluorometer both before and after acidification with HCl (as described in Parsons, 2013).

Stable carbon isotope ($\delta^{13}C$) analysis of POM was carried out at the University of California Davis Stable Isotope Facility. POM filters were freeze-dried and packed in tin capsules prior to analysis of $\delta^{13}C$, as well as total C content using an elemental analyzer isotope ratio mass spectrometer. Long-term standard deviation for these analyses at UC Davis are ±0.2‰ for ^{13}C (UC Davis Stable Isotope lab, https://stableisotopefacility.ucdavis.edu/13cand15n.html', accessed 08.2020).

Absorption spectra for optical characterization of DOM were generated at NIVA by measuring absorption at 1 nm intervals from 200 to 900 nm on a Perkin-Elmer Lambda 40P UV/VIS Spectrophotometer using a cuvette with a 5-cm path length. Absorbance values were blank-corrected (based on Milli-Q blanks), and corrected for potential absorption offset by subtracting mean absorbance between 700 and 900 nm for each sample run (Blough, 2002; Jaffé et al., 2008).

To calculate specific absorption at 254 nm ($SUVA_{254}$) for DOM and POM, absorbance at 254 nm was divided by DOC concentration (Weishaar et al., 2003). E2:E3 was calculated as the ratio between absorbance at 250 nm and 365 nm (De Haan and De Boer, 1987; Peuravuori and Pihlaja, 1997). The spectral slope between S275:S295 (in nm^{-1}) was calculated as the non-linear slope of absorption (Naperian absorption coefficients) vs. wavelength between 275 and 295 nm as described in McGovern et al. (2019).

2.4. Discharge data and residence time

River discharge data were retrieved from the Norwegian watercourse and energy directorate (Norwegian watercourse and energy directorate (NVE), http://sildre.nve.no/, accessed 08.2017 and 07.2018) for the Lundevann monitoring station for the narrow boreal system (58° 40′ 06.1" N, 8° 58' 40.5" E, Agder county) and the Målselvfossen monitoring station for the broad subarctic system (69° 2′ 5.748″ N, 18° 39′ 30.0234″ E, Troms and Finnmark county). Since the Målselvfossen hydrologic monitoring station is located higher up in the catchment, total discharge from the river to the fjord was estimating by scaling up the measured discharge at Målselvfossen (catchment area of 3239 km^2) to the catchment as a whole (catchment area of 5913 km^2).

To gain a coarse estimate of residence time in the study fjords, the volume of the systems was calculated based on data from https://portal.emodnet-bathymetry.eu/(EMODnet Bathymetry Consortium (2018); Thierry et al., 2019) by masking out the land area. The volume of the system was divided by the mean river discharge rates for the study years. It should be noted that this approach does not account for seasonal variability in river discharge and is also likely to represents a substantial overestimate of the true residence time, since salinity stratification and estuarine circulation can allow for rapid offshore transport of buoyant river water. Since the innermost part of the narrow boreal system was not included in the coastal bathymetry data used (where data were only available for the fjord area beyond the narrow and shallow channel connecting the inner fjord to the mid- and outer fjord, we estimated the freshwater residence time in the inner basin by dividing the estimated volume of the surface freshwater layer in the permanently stratified inner fjord by river discharge. The freshwater layer volume was estimated to be 11 million m^3 based on a previously reported estimate for the volume of the uppermost 5 m of the inner fjord, where the halocline depth is typically between 4 and 8 m (Tjomsland and Kroglund, 2010).

2.5. Data treatment and statistical analysis

All statistical analyses were done in R (Version R 3.6.1 GUI 1.70 El Capitan build', R Core Team, 2019). For the narrow boreal system, water chemistry for samples collected at 20 m depth from station B differed strongly from other sites and depths due to the unique characteristics of this site (a deep inner fjord basin with a permanently anoxic brackish deep water layer), and these data were therefore excluded from further analysis. Due to the high number of values below the limit of detection (LOD) in the broad subarctic dataset, ammonium (NH_4) was excluded from further analysis (46.9% of data below detection limit of <5 μg/l), while phosphate (PO_4) non-detects (2.1% below detection limit of <1 μg/l) were replaced by randomly generated values between 0.5*LOD and LOD.

A Principal Component Analysis (PCA) (R library vegan: Oksanen et al., 2019) was carried out on scaled and centered data for a subset of water chemistry and DOM quality variables in order to identify key patterns in water chemistry across both estuaries. Variable selection was based on including the main variables of interest related to nutrient and OM dynamics and limiting inclusion of highly collinear variables. Hierarchical cluster analyses (and heatmap visualization (R library gplots: Warnes et al., 2019)) was carried out independently for each system based on surface water chemistry and DOM quality parameters. These cluster analyses were used to assess the main structuring forces for surface water chemistry in the two river-to-fjord systems, with a particular focus on assessing the role of spatial changes along the river-fjord continuum *vs.* seasonal processes. A hierarchical generalized additive model (HGAM) (R library mgcv: Wood, 2017; see also: Pedersen et al., 2019) was run for each system separately to test for nonlinear functional relationships between water chemistry parameters and salinity under the consideration of different functional shapes. This approach also allowed us to test for conservative mixing patterns in the respective systems. AIC was used for model selection (Johnson and Omland, 2004).

3. Results

3.1. Depth profile

The narrow boreal system (Figs. 1 and 2a) is shallow compared to the broad subarctic system transect (Figs. 1 and 2b), with a steady decline in depth along the fjord transect with the exception of station B, which is located in a deep inner basin of the fjord and separated from the outer fjord by a shallow and narrow channel, forming a boundary with little exchange in the deep waters. This leads to a permanently stratified inner basin with a freshwater layer overlying anoxic brackish waters, and creates unique chemical and biological conditions. This led us to exclude this station from further statistical analyses, although this inner basin represents an interesting case study for future study, and is likely to have important implications for the cycling and fate of riverine OM and nutrients passing through this basin on the way out to sea. In the broad subarctic system, the river station and station A (located on the river delta rim) are shallow, with a relatively sharp increase in depth moving from the river delta and along the fjord transect.

3.2. Riverine discharge, residence time and water chemistry

The volume and seasonal variability of riverine discharge differed between the two estuaries (Fig. S1, Table S3), with higher and more variable discharge in the broad subarctic system. Discharge in 2015/2016 ranged between 1.3 and 140 m^3/s (mean: 12.2 m^3/s) for the narrow boreal system and between 17 and 739 m^3/s (mean: 154 m^3/s) for the broad subarctic system (discharge estimated by upscaling from upstream monitoring station). For the narrow boreal system, we estimated freshwater residence time in the inner basin to be approximately 10 days, and residence time in the remainder of the fjord to be approximately 5 days, suggesting a total residence time of approximately 15 days for this system (based on mean river discharge rates for 2015–2016). Residence time in the broad subarctic fjord for 2015/2016 was estimated to be 5.9 days. Given that these estimates do not take into account salinity stratification (aside for estimates for the inner fjord in the narrow boreal system) or estuarine circulation processes, they are likely to be substantial underestimates of the true freshwater residence times in these fjords. Suggesting, that aside from a longer residence time in the innermost part of the boreal study fjord, residence times are very short (on the order of days) for both the subarctic fjord, and the mid- and outer parts of the boreal study fjord.

Riverine total nutrient (TN, TP) and inorganic nitrogen ($NO_3 + NO_2$, NH_4) concentrations were higher in the narrow boreal system than in the broad subarctic system (Table 2). SiO_2 concentrations were similar between the two systems, while PO_4 concentrations were, on average, nearly 5-fold higher in the surface waters of the subarctic system than the boreal system (Table 2). Mean riverine DOC concentrations were more than 4-fold higher in narrow boreal system (5.5 ± 0.9 mg/L) than at the broad subarctic system (1.2 ± 0.9 mg/L). The subarctic study river had higher seasonal (i.e. between-date) variability in water chemistry than the boreal study river, where water chemistry was generally similar across study dates (Table 2).

3.3. Salinity along the transects

In the narrow boreal system there was a gradual increase in surface water salinity from the innermost riverine to the outermost marine station (Fig. 2c). The river station and subsequent station (B) had the most seasonally stable surface water salinity (<1), while the shallow mid-fjord station C (Fig. 2a) experienced strong differences in salinity between sampling dates.

In the broad subarctic system, fjord surface water salinity differed strongly between sampling dates (Fig. 2d, Table 2). On two occasions, including during spring snowmelt in June 2016, and on a wind-free summer day in August 2016, the fresh surface layer extended to the outermost station, with surface water salinity of <1 more than 15 km from the river outlet (Fig. 2d). For the remaining study dates, fjord surface waters were brackish, with strong between-site and between-date variability in salinity. The variability in fjord surface water salinity was driven primarily by the high seasonality in riverine discharge, the influence of tides (especially for the shallow inner fjord) as well as the degree of wind-induced mixing and strength of stratification. This system experiences much higher variability in river discharge and higher tidal amplitude than the narrow boreal system (Table 1).

In both estuaries, salinity for deep water samples (collected at 20 m, 8 m for station C in the boreal system) was higher than the surface water salinity, even for the most marine stations. In the broad subarctic system the deep-water salinity differed very little between stations and was stable throughout the study period. The deep-water salinity in the narrow boreal system was more variable than at the broad subarctic system. Here, contrasts in salinity between surface and deep-waters were most pronounced at station B (Fig. 2b), reflecting its unique bathymetry, i.e. a deep and nearly fully enclosed and permanently stratified inner basin of the fjord, where river water is delivered to a fresh surface water layer overlying a brackish (and anoxic) deep water layer. There was a declining contrast between deep and surface waters salinity along the transect toward the outer fjord.

3.4. Spatial and seasonal patterns in water chemistry

In the narrow boreal system, surface water chemistry exhibited directional changes along the river-inner fjord-outer fjord gradient and was distinct from water chemistry in the deep water samples (typically

Table 2
Mean values (and standard deviation) for the 2015/2016 study period for selected water chemistry variables (including Chl a and $SUVA_{254}$). Values for river water, surface and deep fjord water are shown for each of the two study systems. Molar concentrations are also presented for DOC and nutrients (to facilitate comparison). Data for E2:E3, S275-295 and $\delta^{13}C$ of POM are reported in Table S2.

		Narrow boreal system			Broad subarctic system		
		river station	fjord stations		river station	fjord stations	
		surface	surface	deep	surface	surface	deep
Salinity	mean	1.4	15.9	29.2	0	10.1	32.8
	SD	1.3	9.3	2.4	0	10.2	0.5
DOC in mg C/l (μmol C/l)	mean	5.5 (458)	3.6 (300)	1.8 (150)	1.2 (100)	1.3 (108)	1.3 (108)
	SD	0.9 (749)	1.3 (108)	0.4 (33)	0.2 (17)	0.3 (25)	0.2 (17)
TN in μg N/l (μmol N/l)	mean	404.0 (29)	272.6 (19)	182.5 (13)	218.6 (16)	137.9 (10)	149.9 (11)
	SD	85.0 (6)	87.1 (6)	29.9 (2)	97.7 (7)	49.9 (4)	30.2 (2)
TP in μg P/l (μmol P/l)	mean	7.6 (0.2)	10.6 (0.3)	14.5 (0.5)	5.4 (0.2)	9.0 (0.3)	19.3 (0.6)
	SD	2.4 (0.08)	3.1 (0.1)	3.4 (0.1)	3.2 (0.1)	6.8 (0.2)	8.9 (0.3)
SiO_2 in μg/l (μmol Si/l)	mean	2334.0 (83)	1109 (39)	170.8 (6)	2181.0 (78)	1569.0 (56)	113.9 (4)
	SD	598.7 (21)	947.4 (34)	84.9 (3)	274.9 (10)	656.3 (23)	69.5 (2)
PO_4 in μg P/l (μmol P/l)	mean	1.8 (0.06)	2.68 (0.09)	8.0 (0.3)	8.8 (0.3)	8.2 (0.3)	9.7 (0.3)
	SD	0.8 (0.03)	2.2 (0.07)	7.7 (0.2)	4.4 (0.01)	4.4 (0.1)	4.0 (0.1)
$NO_3 + NO_2$ in μg N/l (μmol N/l)	mean	139.3 (10)	58.5 (4)	30.1 (2)	59.4 (4)	46.1 (3)	33.3 (2)
	SD	65.3 (5)	60.9 (4)	20.7 (1)	34.4 (2)	25.1 (2)	33.8 (2)
$SUVA_{254}$ in m^2/g C	mean	3.9	2.8	1.6	3.1	2.4	1.1
	SD	0.4	0.9	0.2	0.7	0.6	0.3
Chl a in mg/m^3	mean	1.0	1.4	0.7	0.3	0.2	1.2
	SD	0.7	1.0	0.5	0.3	0.2	1.2

collected from 20 m). The river and inner- and mid-fjord surface waters were characterized by higher DOC, $SUVA_{254}$, TN, NO_3+NO_2, NH_4 and SiO_2 and lower PO_4, TP, $\delta^{13}C$ of POM and spectral slope (S275:295) than the outer fjord surface waters and deep waters along the transect (Table 2, Table S2, Fig. S4, Fig. S6). The brackish anoxic deep water at Station B was characterized by extremely high concentrations of NH_4 and PO_4 (and to a lesser degree SiO_2) highlighting the unique biogeochemistry of this inner fjord basin. These spatial patterns in water chemistry were relatively consistent across study dates.

In the broad subarctic system, spatial patterns in nutrient concentrations were less clear and often differed depending on season. As also observed in the narrow boreal system, SiO_2 concentrations were much higher in the river and fjord surface waters than in the deep fjord waters. This was also the case for $NO_3 + NO_2$, although for sampling dates in winter (March 2016) and late autumn (November 2016) concentrations were relatively similar for both sampling depths along the study transect. Riverine concentrations of DOC and NH_4 were often similar to concentrations observed in deep outer fjord marine waters, although this also varied with sampling date (e.g. riverine NH_4 concentrations were higher than marine concentrations during spring 2016 but lower than marine concentrations in June 2016). PO_4 concentrations were generally higher in deep marine waters, although during periods of high river flow, PO_4 concentrations in the river and inner fjord surface waters were higher than in outer fjord and deep waters. The river and brackish fjord surface waters tended to have higher $SUVA_{254}$ and lower $\delta^{13}C$ of POM and S275:295 (Table 2, Table S2, Fig. S5, Fig. S7) than the marine-

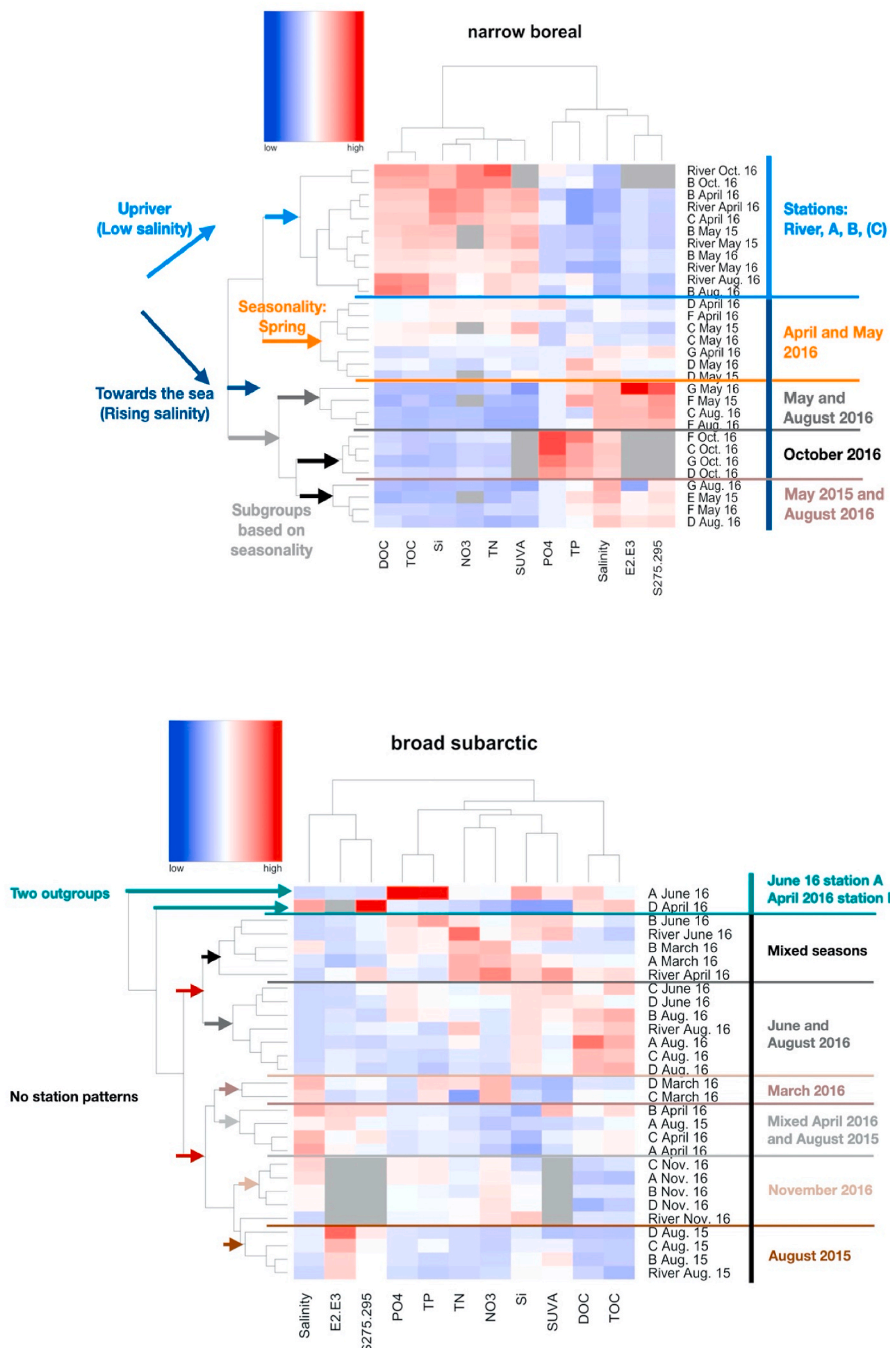

Fig. 3. Heatmap showing results of correlation analysis and hierarchical multivariate clustering for surface water chemistry data for the two study systems. Cells are shaded grey where data were not available.

influenced deeper waters, as was also observed for the narrow boreal system, suggesting similar contrasts between freshwater and marine OM composition.

Within sampling date, spatial patterns in surface water chemistry generally reflected salinity patterns, with similar surface water chemistry across the whole transect for sampling dates where the river plume extended throughout the entire fjord (June and August 2016), and changes in surface water chemistry along the transect on sampling dates where a horizontal salinity gradient was present.

3.5. Structuring forces

The horizontal gradient in salinity from river to outer fjord was the major structuring driver of surface water chemistry at the narrow boreal system, including for nutrient and DOC concentrations and OM properties (Fig. 3). Here the freshwater dominated stations (A and B) were distinct from the brackish water stations (D to G), with station C clustering with freshwater or brackish water stations depending on sampling date. The strongly freshwater influenced stations were characterized by high OC, Si, NO_3+ NO_2 and TN concentrations, while the outer fjord stations were characterized by higher salinity, as well as higher TP concentrations. OM absorption properties also differed between these clusters, with higher $SUVA_{254}$ in inner fjord surface waters, and higher E2:E3 and S275:295 in the outer fjord. The water chemistry at the brackish water stations (C-G) clustered further based on seasonality, with apparent between-cluster differences in nutrient concentrations.

In contrast, surface water chemistry (including OM properties) in the broad subarctic system do not cluster according to station but rather cluster broadly according to sampling date (Fig. 3), with river water samples often clustering with fjord surface water from the same date. Clustering was driven by strong between date differences in salinity, nutrient and DOC concentrations and OM properties, indicating a high degree of seasonal variability in these variables. Although there were several sampling dates with low surface water salinity across the entire fjord, these dates did not always cluster together, due to strong between-date differences in other water chemistry variables (including low vs. high DOC and NO_3 + NO_2 and differences in OM properties), further highlighting the importance of seasonality in discharge, river water chemistry, and marine nutrient concentrations in driving water chemistry in this system.

3.6. Patterns in nutrients and organic matter along the study transects

The narrow boreal system had higher variability in water chemistry and OM related variables along the salinity gradient (Fig. 4: PC 1) than the broad subarctic system. The surface water chemistry differed considerably between the two fjords and also exhibited higher within-system variability than observed for deep water. Salinity, and several variables closely linked to the degree of freshwater influence (i.e. pH, SiO_2, $SUVA_{254}$, S275-295, $\delta^{13}C$ of POM, NO_3+ NO_2) were strongly associated with PC1 (explained 52% of the total variance in the dataset), while PC2 (explained 14% of the variance) was associated with Chl a, DOC and PO_4 concentrations. Deep-water samples separated from surface water samples primarily along PC1, while the surface water from the two study systems primarily separating along PC2, apparently reflecting differences in DOC and Chl a (higher in the narrow boreal system), and PO_4 (higher in the broad subarctic system). There was considerable overlap between study systems for deep water chemistry including OM absorption properties. The broader spread of the data from the narrow boreal system surface waters along PC1 reflects the consistent horizontal patterns in salinity and surface water chemistry along this study transect, where salinity (and pH) increases alongside decreasing Si and DOC concentrations, and there is a gradual shift in from terrestrial to marine OM (as indicated by $SUVA_{254}$, $\delta^{13}C$ as well as S275-295). The narrower spread of surface water data for the broad subarctic system along PC1 once again indicates that salinity is not the

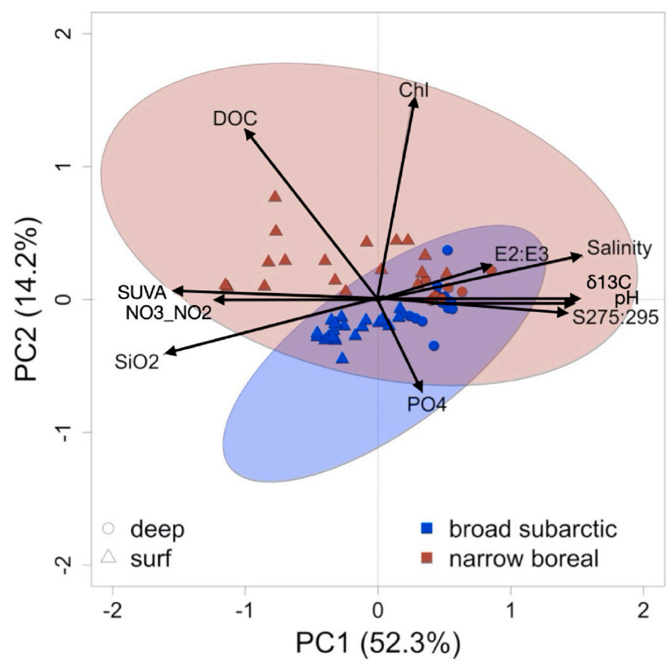

Fig. 4. Principal component analysis (PCA) of key water chemistry variables and DOM indicators for the narrow boreal system (red points and ellipse) and the broad subarctic system (blue points and ellipse), shape of the data points indicates sampling depth. Ellipses are based on the SD with a 95% confidence limit. (For interpretation of the references to colour in this figure legend, the reader is referred to the Web version of this article.)

primary driver of surface water chemistry in this system. SiO_2 and NO_3+ NO_2 was negatively with salinity in both systems, suggesting that both rivers act as a source of these nutrients to the marine environment. The lack of association between PO_4 and with salinity suggests that these rivers do not acting as a strong source of phosphorus to the adjacent marine waters. The spread of deep-water data along PC2 is more pronounced in the broad subarctic system, likely linked to seasonal changes in SiO_2 and Chl a.

3.7. Mixing patterns across seasons

Nutrient and DOM patterns differed between the two systems both across the freshwater-marine transect and between the seasons (Fig. 5, Fig. 6, Table S4). There were strong changes in nutrient concentrations and OM characteristics along the transect in the narrow boreal system, whereas nutrient concentrations and OM characteristics were more similar along the transect in the broad subarctic system but exhibited higher seasonal variability.

Hierarchical GAM analysis revealed consistent linear relationships between salinity and DOC, $\delta^{13}C$ of POM and TP on most sampling dates for the narrow boreal system, indicating conservative mixing (Fig. 5a, Figs. S2b and c, Table S4a), while $SUVA_{254}$ exhibited conservative (or mostly conservative) mixing patterns on some, but not all, study dates (Fig. 5b). In the broad subarctic system, only SiO_2 exhibited conservative mixing patterns on all sampling dates, while $SUVA_{254}$ and E2:E3 were linearly related to salinity on at least some sampling occasions (Fig. 6b,d, Fig. S3d, Table S4b). In the narrow boreal system, linear (and near-linear) changes in DOC, $\delta^{13}C$ POM and $SUVA_{254}$ with salinity indicate that conservative mixing is the major and dominant driving force behind the OM quantity and quality in the system. While the decrease in $SUVA_{254}$ along the study gradient indicates a shift from more humic DOM of terrestrial origin toward marine DOM, the increase in $\delta^{13}C$ of POM from the inner to outer fjord (Fig S2, Table S4a) indicates a similar shift in dominance from terrestrial to marine POM. This

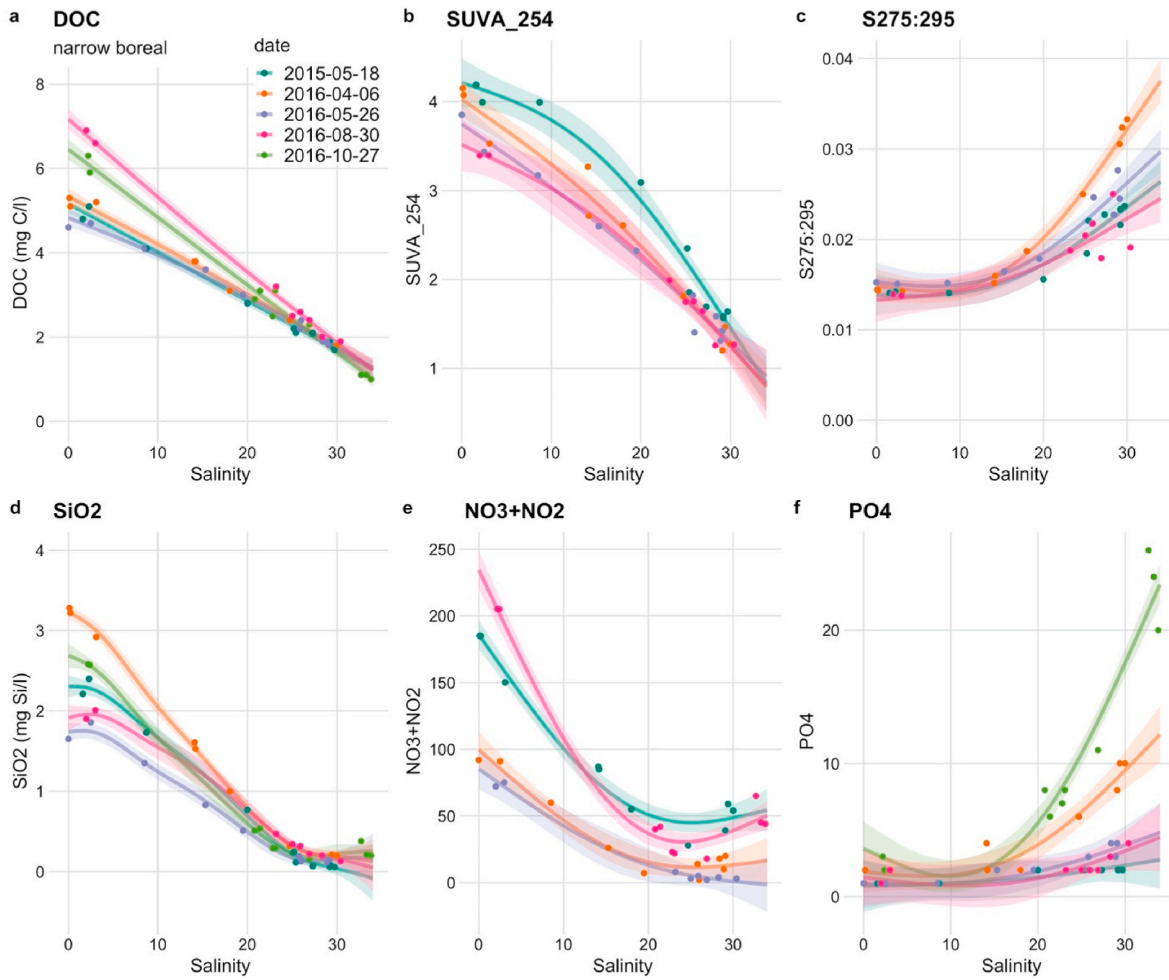

Fig. 5. Hierarchical generalized additive (HGAM) models for DOC, SUVA254, S275-295, SiO2, NO3 + NO2, and PO4 based on data from both depths for the narrow boreal system. Straight linear responses between a variable and salinity indicate conservative mixing patterns without further influential outside effects. Seasonally divergent values (e.g. between-date differences in chemistry of freshwater or marine 'end members') are indicated by seasonally different intercepts (at salinity of 0 for the river and at the maximum measured salinity for marine water). Seasonally-independent processes (mostly chemical/physical) are reflected in response curves that are similar between seasons. Seasonally-dependent processes (including biological activity, but also chemical processes) are reflected in seasonally divergent response curves. See Table S4 for details on the models, and Fig. S2 for HGAM model plots for additional variables.

conservative mixing pattern is only broken during one season (May 2015), where there is a deviation towards higher $\delta^{13}C$ at lower salinities, suggesting a stronger seasonal contribution of phytoplankton to the POM pool. The spectral slope of DOM (S275-295; Fig. 5c, Table S4a), increases non-linearly along the gradient, with relatively stable values below ~15, followed by a seasonally dependent increase, with higher marine S275-295 values in samples collected in April and May of 2016.

Physical mixing also plays a key role in shaping nutrient concentrations along the narrow boreal system, where concentration differences between the river and the receiving marine waters drive a negative relationship between salinity and $NO_3 + NO_2$ (and TN) as well as SiO_2, and a positive relationship between salinity and PO_4. However, the complex non-linear relationships between salinity and dissolved inorganic nutrient concentrations (e.g. the steep non-linear decline in $NO_3 + NO_2$ with salinity; Fig. 5e) and S275-295 (Fig. 5c), and seasonal changes in response curves indicate that biological or chemical processes are also shaping nutrient and DOM patterns along the transect (Fig. 5c, e, f, Table S4a). Meanwhile, strong seasonality in water chemistry of riverine and marine 'end members' also point to seasonal changes in riverine and marine nutrient and OM supply to the study fjords (Fig. 5a, e, f).

In the broad subarctic system, SiO_2 (Fig. 6d) is the only water chemistry variable measured that consistently exhibits strong conservative mixing patterns, although $SUVA_{254}$ (Fig. 6b) decreases linearly with salinity on 3 of 5 sampling dates where data are available. The reduced importance of conservative mixing in this system compared to the narrow boreal system is linked to the lack of strong contrast between riverine and marine water chemistry from several of the variables of interest. Furthermore, for several sampling dates, a lack of data at intermediate salinities increases uncertainty related to the shape of response curves (Fig. 6) and makes it challenging to accurately assess conservative mixing patterns and/or non-linear response curves. Sampling date, rather than salinity, seems to be the main driver of patterns in DOC (Fig. 6a, Table S4b), NO_3+ NO_2 and TN (Fig. 6e, Fig. S3a, Table S4b), PO_4 and TP (Fig. 6d, Fig. S3b, Table S4b). In particular, strong seasonal differences in concentrations and response curves for NO_3+ NO_2 indicate seasonal changes in riverine and marine nutrient supply, as well as in biological uptake rates. PO_4 concentrations in this system varied strongly between date, with distinctly high concentrations occasionally observed in river water and the freshwater surface layer in the fjord as well as in deep marine waters. The overall concentration and patterns of DOC differ strongly between date, however, as observed for the narrow boreal system, $SUVA_{254}$ tends to decrease with salinity, while S275-295 increases, with the strongest increase observed at higher salinities (Fig. 6c). An increase in $\delta^{13}C$ of POM (Fig. S3c, Table S4b) is also observed with increasing salinity in most seasons, indicating a shift

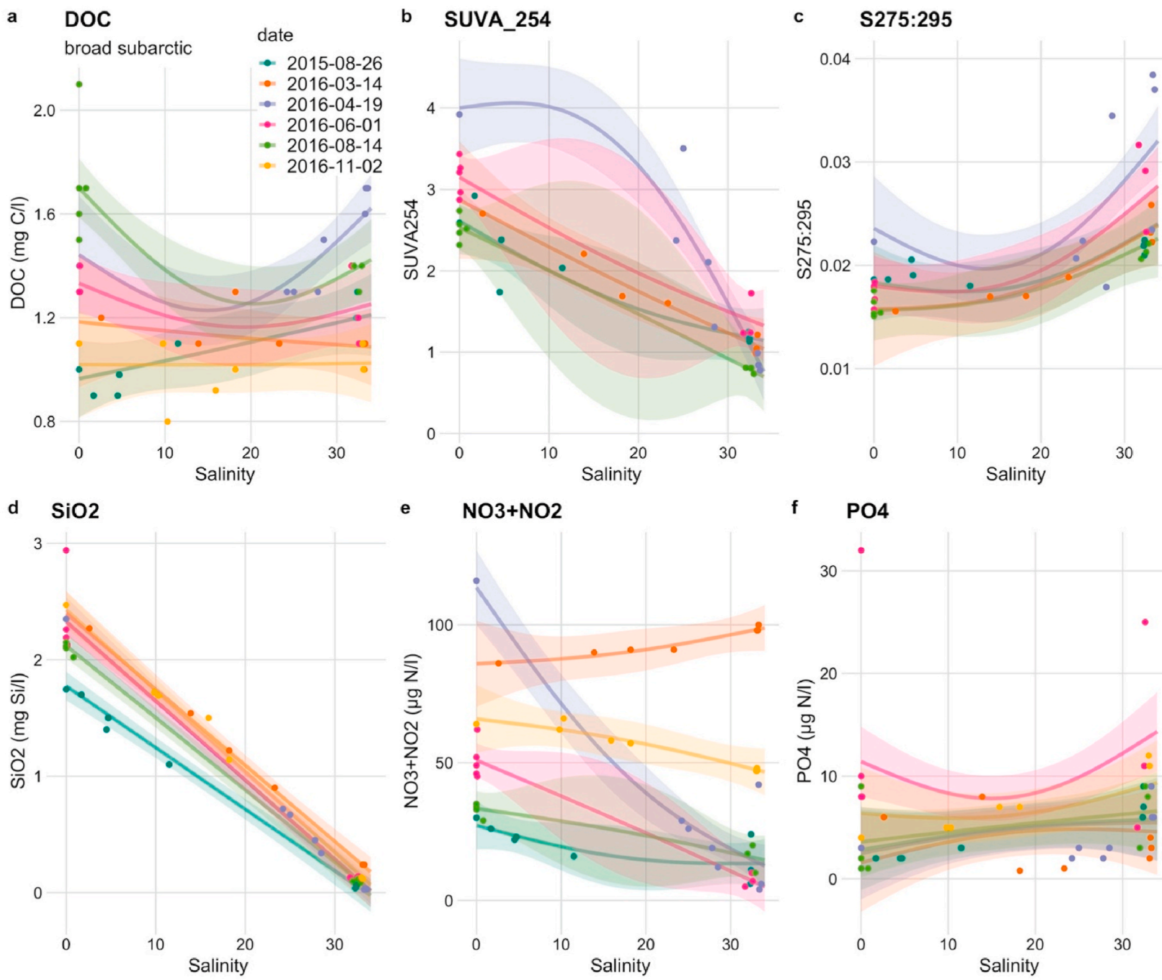

Fig. 6. Hierarchical generalized additive (HGAM) models based on data from both depths for the broad subarctic system. See Fig. 5 caption for more details. For details on the models, see Table S4, and see Fig. S3 for HGAM model plots for additional variables.

from terrestrial to marine POM. However unlike in the narrow boreal system where $\delta^{13}C$ was typically linearly related to salinity, in the broad boreal system, non-linear response curves were typically observed, with differences in concentration and response curves between sampling dates/seasons.

4. Discussion

Transfer of organic matter and nutrients along the freshwater-marine continuum is based on a combination of site-specific attributes both in terms of catchment properties, seasonal changes in OM and nutrient delivery to the coast, as well as coastal morphometry and hydrodynamics. In the current study, we found that while catchment properties and seasonality shaped the geochemistry of freshwater and marine 'end members'; fjord morphometry was the main driver for spatial patterns in salinity, OM and nutrients and for transfer of terrestrial material along the study gradients.

4.1. Catchment properties affect nutrient and OM levels

The different properties of the two systems - one estuary located in a nearly pristine mountainous subarctic environment and the other in a boreal, forested catchment with stronger anthropogenic influences - are clearly reflected in the nutrient and DOC concentrations in the rivers and along the transects. The higher concentrations of $NO_3 + NO_2$ and TN in the river and fjord surfaces waters of the narrow boreal system to some degree reflect anthropogenic sources in the drainage basin, including the higher atmospheric deposition of N in southern Norway compared to northern Norway, while the higher TN also likely reflects high concentrations of organic N associated with the higher levels of DOM_{terr} in this river (Deininger et al., 2020). The higher concentrations of SiO_2 and PO_4 in river and fjord surface waters in the broad subarctic surface waters likely reflect local geology (including presence of phosphate-rich bedrock) and weathering/erosion, including in the higher elevation poorly-vegetated parts of the catchment (Kaste et al., 2018). In addition, the subarctic river has a considerably larger catchment area than the boreal river (5913 vs. 408 km^2) and stronger seasonality in discharge, with pronounced seasonal snowmelt floods due to its subarctic location (Avagyan et al., 2016).

The two systems differ considerably in DOC concentrations and DOM characteristics. The three-fold lower concentrations of DOC in the subarctic river and fjord surface waters compared to the boreal system reflect differences in catchment properties, with higher forest and wetland cover in the boreal site, as well as differences in land-use and precipitation between the two sites (Kaste et al., 2018). Differences in DOM absorption properties between the two study rivers also point to differences in OM composition, including a stronger contribution of OM with high molecular weight (lower S275-295) and high aromatic content (higher $SUVA_{254}$) (Hansen et al., 2016; Weishaar et al., 2003) in the boreal river, and lower molecular weight OM (higher S275-295; Hansen et al., 2016) in the subarctic river, potentially indicating higher rates of photochemical degradation of riverine DOM in this system (Hansen et al., 2016). Higher photochemical degradation of DOM in the subarctic river could potentially be linked to the large lakes present in the catchment and clear waters, which would increase residence time as well as light exposure of riverine DOM (Kothawala et al., 2021).

Differences in seasonal catchment processes (including discharge) between the two study systems are also reflected in the higher seasonal variability in riverine concentrations of nutrients (except for SiO_2), DOC and OM absorption properties in the subarctic river compared to the boreal river. These results are consistent with other studies that have pointed to particularly strong seasonality in water chemistry and OM properties for high latitude rivers (Finlay et al., 2006; Holmes et al., 2013).

4.2. Fjord morphometry and seasonality shape salinity and stratification

Compared to coastal areas that have limited exchange with open marine waters (such as our narrow boreal fjord system), in an open coastal system with a high degree of exchange with offshore marine waters (such as our broad subarctic system), strong dilution of freshwater and terrestrial nutrients and DOM_{terr} can lead to reduced concentrations, highlighting the role of morphometry in shaping the transport and fate of riverine nutrients and OM in the marine environment. However, even in broad and open fjords, strong estuarine circulation and salinity stratification, particularly during periods of high river discharge can lead to rapid offshore transport of freshwater and terrestrial material (Asmala et al., 2016). In the current study, the morphometry of the estuary and fjord basin was a major determinant of salinity, nutrient and organic matter dynamics.

The narrow and more sheltered boreal system with its low tidal amplitude is characterized by a gradual decline in salinity along the transect and comparably low variability in salinity between sampling dates. In this estuary, nutrient and DOC concentrations cluster according to sampling stations and salinity and are only modestly impacted by seasonality. In contrast, the subarctic system, with its broad and open fjord, is strongly affected by estuarine circulation and tidal cycles pushing seawater far up into the estuary, equalizing the salinity levels across the gradient via mixing. However, during periods of high river discharge, freshwater inputs from the large subarctic river can lead to a buoyant freshwater or brackish river plume that can 'flood' the surface waters of the subarctic fjord with freshwater, resulting in a similar (but directionally opposite) equalizing effect on surface water salinity in the system, and restricting mixing and impacting availability of light, nutrients and DOM in the upper water column. These between system differences in mixing and salinity are also reflected in fjord water chemistry, with the narrow boreal system exhibiting strong horizontal gradients and the broad subarctic system exhibiting strong vertical gradients in nutrient and OM patterns.

Considering the high seasonality in river discharge combined with the shorter terrestrial and marine growth season at high latitudes, the lack of clear seasonal patterns in measured nutrient concentrations and OM in in the broad subarctic system was surprising. Even during a high flow event (June 2016, Fig. S1), the measured water chemistry was generally similar to the other dates, although these samples were collected during the late freshet period, when dilution processes can lead to much lower DOC and nutrient concentrations than during the early phases of the spring snowmelt period (Finlay et al., 2006; McClelland et al., 2014). However, more generally, this also reflects the lack of a strong contrast in OC and nutrient concentrations between the river and the receiving marine waters, such that changes in discharge impact salinity, and may impact the relative contribution of terrestrial vs. marine sources of nutrients or OC, but may not necessarily have a strong impact on total nutrient concentrations.

4.3. Conservative and non-conservative mixing of nutrients and DOM

Conservative mixing patterns are more likely to occur where nutrient and DOC concentrations are high since losses through flocculation and sedimentation may be small in comparison with total concentrations (Sholkovitz et al., 1978). Similarly, high concentrations of nutrients and DOC paired with relatively low levels of biological uptake (e.g. due to limitation by light or other nutrients or seasonal changes in biological activity) would also be expected to lead to relatively low nutrient uptake compared to total concentrations. On the other hand, longer residence time of freshwater in estuaries (e.g. due to lack of exchange with open marine waters and/or wind-induced mixing that limits the development of a buoyant river plume) can lead to higher removal and transformation of riverine OM and nutrients along the freshwater-marine gradient (e.g. through sedimentation, biological uptake, and/or photochemical and microbial degradation; Voss et al., 2021; Bianchi et al., 2020).

While SiO_2 mixes conservatively in the broad subarctic system and exhibits a near-linear decline in the narrow boreal system, $NO_3 + NO_2$ and PO_4 do not. In the narrow boreal system, the apparent conservative mixing of TP, and the gradual decline in TN with salinity, likely reflect high concentrations of riverine dissolved organic N and P in fresh and brackish waters, as well as changing contribution of particulate nutrients to the TN and TP pool along the study transect. These changes could mask underlying non-linear changes in $NO_3 + NO_2$ and PO_4 which are generally present at low concentrations.

Season had only a minor effect on overall concentrations of SiO_2, TP and PO_4 in the broad subarctic system, indicating relatively consistent supply of these nutrients to the fjord system from both the river (for SiO_2 and PO_4) and deeper marine waters (for PO_4). In contrast, the strong seasonality in $NO_3 + NO_2$ concentrations and their relationship to salinity highlights the importance of seasonal changes in availability and biological uptake. For example, concentrations were high in both the river and marine waters during the late autumn and winter when biological uptake by terrestrial and aquatic primary producers is low (Sponseller et al., 2014) and when mixing and advection processes deliver nutrients from deeper marine waters to surface and nearshore waters (e.g. Wassmann et al., 1996). Strong evidence of higher biological uptake along the salinity gradient during the spring and summer growth season has also been observed in several other studies in northern estuarine systems (Humborg et al., 2003; Ylöstalo et al., 2016). The lack of seasonality in marine SiO_2 concentrations in the broad subarctic system suggests that concentrations are sufficiently high in these nearshore coastal waters that changes due to biological uptake (e.g. diatoms that are limited by other factors than silicate) or other physical removal processes become negligible. Further, the low water residence times in these fjords may also limit our ability to detect biological uptake along the study transects.

In the narrow boreal system, both $NO_3 + NO_2$ and SiO_2 decline with increasing salinity, and there is an effect of seasonality on riverine transport of nutrients and their transfer to the ocean, with seasonal changes in riverine concentrations setting the stage for surface water concentrations throughout the fjord, and evidence of biological uptake along the salinity gradient for these nutrients for all sampling dates, with SiO_2 concentrations that typically plateau at very low values at approximately 25, and $NO_3 + NO_2$ concentrations that reach very low levels, especially during periods of high primary productivity (e.g. during spring 2016). For PO_4, concentrations remain low between the river and intermediate salinities, with increasing concentrations often observed above ~15, indicating P-limitation and high biological uptake of marine PO_4 in the inner and mid-fjord surface waters.

The OM dynamics of the two systems behave very differently: DOC concentrations are higher at the narrow boreal system, where conservative mixing is observed. Chlorophyll concentrations are also higher in the boreal system, likely reflecting the higher nutrient concentrations in the region, but also the highly seasonal nature of primary production in the subarctic system, where periods of high productivity may have been missed by our sampling campaigns.

While DOC concentrations and $\delta^{13}C$ of POM at the narrow boreal system typically decline linearly, reflecting riverine inputs and a gradual shift in source of the DOM and POM towards marine sources, S275:295 changes non-linearly along the transect. Increasing S275:S295 is a common proxy for photochemically-induced reduction in molecular weight (Twardowski et al., 2004), although microbial degradation or flocculation processes may also impact the molecular weight of the remaining DOM in a non-linear way (Boyd and Osburn, 2004; Sholkovitz et al., 1978; Twardowski et al., 2004). The variation in S275:S295 in the broad subarctic system across seasons co-occur with the $\delta^{13}C$ variability and reflects seasonality in the relative contribution of terrestrial and marine (phytoplankton-derived) POM. This high variability in DOM molecular weight and $\delta^{13}C$ of POM likely reflect inputs or *in situ* production of different sources of OM across the seasons, e.g. due to phytoplankton blooms or progressive snowmelt patterns that drain different parts of the catchment area or soil depths at different times (Avagyan et al., 2016).

Overall, DOM (and POM) composition in the narrow boreal system are structured primarily by riverine inputs of terrestrial OM. This suggests that effects on the biota (e.g. visibility conditions, contaminant loads) will differ strongly along the gradient, independent of season. In the broad subarctic system, low DOC concentrations in the river limit the impact of river inputs on OM dynamics in the system, with DOM and POM primarily responding to local seasonal phytoplankton blooms and spring freshet, reflected in the diverging response curves according to season. However, other studies in high latitude rivers focusing on riverine DOC fluxes to the coast have highlighted the potential for the spring snowmelt period to deliver up to half of total annual OC-fluxes over a period of only a few weeks (Finlay et al., 2006; Holmes et al., 2013), and to deliver DOM that is particularly labile relative to the higher molecular weight DOM that is typically observed in other seasons (Kaiser et al., 2017). Since DOC mixing patterns were purely conservative at the narrow boreal system, the effect of seasonal phytoplankton blooms on the total DOC pool appears to be small. Thus, while overall autochthonous production may be higher in the narrow boreal system, the relative importance of autochthonous production for driving OM dynamics was higher in the broad subarctic system.

In both systems OM properties for deep water at the marine stations were very similar to each other, and were also distinct from their respective surface water systems. This suggests a decoupling of surface and deep waters, with deep waters being dominated by inflow from the Norwegian Coastal Current. The deep water in the broad subarctic system is, however, more similar to its surface system than is the case in narrow boreal system. This is likely due to the lack of contrast in nutrient and OC concentrations between river and marine water. Interestingly, $\delta^{13}C$ of POM differs strongly between surface and deep water in both estuaries, despite the fact that POM sinks out and should thus connect surface to deep waters. In addition to loss through sedimentation, POM is a preferred food source for heterotrophic bacteria (Tranvik and Sieburth, 1989), and is also utilized by grazers and filter-feeders (Williams et al., 2014), providing a pathway for uptake into pelagic and benthic food webs. $\delta^{13}C$ values of POM can also shift through heterotrophic processing or the contribution to the POM pool by bacteria. These differences could also reflect contribution to the deep-water POM by high $\delta^{13}C$ particulate matter from subsurface phytoplankton blooms and advected phytoplankton from offshore waters. In shallow waters benthic organisms and sediments may also be important sources of DOC to the overlying water column (Lønborg et al., 2020).

4.4. Climate change and coastal darkening

Climate change in Europe will be reflected in increases in heavy rainfall and changes in timing and magnitude of spring snow melt that can lead to flooding events as well as droughts (Seneviratne et al., 2012). These changes have the potential to alter the mobilization and transport of DOM_{terr} and nutrients from land to sea, with climate and catchment properties interacting to define what will occur downstream. Flood events or shifts between droughts and floods may lead to intense pulsed inputs of DOM_{terr} that can act as a stressor for impacted coastal ecosystems (Paczkowska et al., 2020). While no such extreme events were captured in the current study, previous studies, including during spring snowmelt floods, have pointed to the importance of these extreme events for land-ocean OM and nutrient fluxes and their potential impacts on downstream coastal ecosystems (Paczkowska et al., 2020; Stepanauskas et al., 2000; Vidon et al., 2008).

Given documented increases in inputs of DOM_{terr} to northern coastal waters, including along the Norwegian coast, it is particularly important to understand the potential consequences of these inputs for coastal ecosystems (Frigstad et al., 2020). While increased DOM_{terr} is expected to increase coastal light attenuation ("coastal darkening"; Opdal et al., 2019; Aksnes et al., 2009), these inputs are also a source of OC and OM-associated nutrients to coastal waters and sediments, with a range of documented and potential impacts on coastal pelagic and benthic ecosystems (e.g. McGovern et al., 2019; Opdal et al., 2019; Paczkowska et al., 2020). In systems where OC and nutrient concentrations are already high, such as in the narrow boreal system, increased DOM_{terr} may negatively impact phytoplankton abundance and community composition through shading and may allow bacteria to outcompete phytoplankton for nutrients (Paczkowska et al., 2020; Sipler et al., 2017; Vallières et al., 2008). This can lead to a shift in the balance between heterotrophy and autotrophy, with implications for CO_2 balance of coastal waters (Bauer et al., 2013; Paczkowska et al., 2020). However, in waters where OC and nutrient concentrations are currently low, increased DOM_{terr} inputs could also have a positive effect on primary productivity, where light availability is still sufficient for growth and DOM_{terr}-associated nutrients can mineralized and made available for uptake by primary producers (Paczkowska et al., 2020; Vähätalo et al., 2011).

5. Conclusions

The comparison of the two river-fjord systems revealed that while inputs of nutrients and OM_{terr} depend on catchment properties and river discharge, transport and fate of terrestrial OM and nutrients along the freshwater-marine continuum depend strongly on the morphometry of the system, a factor that often overrides the importance of seasonal patterns in our dataset. In the narrow boreal system, there are more gradual directional shifts in nutrient and DOC concentrations and POM properties from the riverine to the marine system. Limited connectivity with the open marine system paired with the higher riverine nutrient and OC concentrations (based on catchment attributes) mean that conservative mixing patterns dominate in this system, although biological uptake of riverine $NO_3 + NO_2$ and advected marine PO_4 was also an important driver of inorganic N and P patterns along the study transect. In the broad subarctic system, a lack of contrast in OC and nutrient concentrations between the river and marine system paired with complex mixing and stratification patterns creates a less structured transect, where vertical differences in water chemistry were much more pronounced than horizontal or seasonal differences, and where conservative mixing was only observed for SiO_2. Although Chl a was generally higher in the narrow boreal system, terrestrial OM dominated the DOM and POM pool in fjord surface waters, while in the subarctic system, despite lower Chl a concentrations, OM of marine origin tended to dominate the fjord OM pool, due to lower riverine inputs of OM from this relatively carbon-poor mountainous catchment. Deep waters in general differed from surface waters but were similar across study systems, likely reflecting inflow of water from the Norwegian Coastal Current at both locations.

Despite the strong differences between the two study systems, we found that there were several drivers and patterns that were common to both systems. Rivers were sources of SiO_2, inorganic N and highly aromatic DOM to the coastal environment, and advected marine waters were a source of PO_4 and low molecular weight/photochemically-degraded DOM. Finally, the contrasts between these systems, as well as the spatial and seasonal dynamics within these systems also provided concrete examples of how catchment properties, hydrology, fjord morphology and seasonality interact to shape fluxes, distribution and fate of terrestrial nutrients and OM in the coastal environment.

Credit authorship contribution statement

Sabrina Schultze: Investigation, Writing – original draft, Visualization, Conceptualization, Formal analysis. **Tom Andersen:** Writing – review & editing, Supervision, Formal analysis. **Dag O. Hessen:** Writing – review & editing, Supervision. **Anders Ruus:** Writing – review & editing, Investigation, Funding acquisition, Conceptualization. **Katrine Borgå:** Conceptualization, Investigation, Supervision, Writing – review & editing. **Amanda E. Poste:** Writing – review & editing, Supervision, Project administration, Methodology, Investigation, Funding acquisition, Formal analysis, Conceptualization.

Declaration of competing interest

The authors declare that they have no known competing financial interests or personal relationships that could have appeared to influence the work reported in this paper.

Acknowledgements

This work was based on a research collaboration on land-ocean interactions supported by the Department of Biosciences at the University of Oslo and the Norwegian Institute for Water Research (NIVA). Field and lab work was supported by NIVA's Strategic Institute Programme on Land-Ocean Interactions and the Fram Centre's Flagship programme for "Hazardous substances: effects on ecosystems and human health". We thank many colleagues who contributed to this work, including: Lena Seuthe, Sebastiaan Koppelle and Guttorm Christensen: contributions to study design, field and lab work; Jarle Håvardstun: field work, Anne-Luise Ribeiro, Cathrine Skaar Hoel, Tina Brytensen: filtration, sample processing, lab analysis; Espen Lund: DOM absorbance analysis; Maeve McGovern: data processing for absorption spectra and chlorophyll analyses; Pernilla Carlsson for help with lab analyses; and Jan David Heuschele for help with the visual abstract.

Appendix A. Supplementary data

Supplementary data to this article can be found online at https://doi.org/10.1016/j.ecss.2022.107831.

References

Aksnes, D.L., Dupont, N., Staby, A., Fiksen, Ø., Kaartvedt, S., Aure, J., 2009. Coastal water darkening and implications for mesopelagic regime shifts in Norwegian fjords. Mar. Ecol. Prog. Ser. 387, 39–49.
Arnold, W.R., Cotsifas, J.S., Smith, D.S., Le Page, S., Gruenthal, K.M., 2009. A comparison of the copper sensitivity of two economically important saltwater mussel species and a review of previously reported copper toxicity data for mussels: important implications for determining future ambient copper saltwater criteria in the USA. Environ. Toxicol. 24, 618–628.
Asmala, E., Autio, R., Kaartokallio, H., Pitkänen, L., Stedmon, C., Thomas, D., 2013. Bioavailability of riverine dissolved organic matter in three Baltic Sea estuaries and the effect of catchment land use. Biogeosciences 10, 6969–6986.
Asmala, E., Bowers, D.G., Autio, R., Kaartokallio, H., Thomas, D.N., 2014. Qualitative changes of riverine dissolved organic matter at low salinities due to flocculation. J. Geophys. Res.: Biogeosciences 119, 1919–1933.
Asmala, E., Haraguchi, L., Jakobsen, H.H., Massicotte, P., Carstensen, J., 2018. Nutrient availability as major driver of phytoplankton-derived dissolved organic matter transformation in coastal environment. Biogeochemistry 137, 93–104.
Asmala, E., Kaartokallio, H., Carstensen, J., Thomas, D.N., 2016. Variation in riverine inputs affect dissolved organic matter characteristics throughout the estuarine gradient. Front. Mar. Sci. 2, 125.
Avagyan, A., Runkle, B.R.K., Hennings, N., Haupt, H., Virtanen, T., Kutzbach, L., 2016. Dissolved organic matter dynamics during the spring snowmelt at a boreal river valley mire complex in Northwest Russia. Hydrol. Process. 30, 1727–1741.
Bartels, P., Hirsch, P.E., Svanbäck, R., Eklöv, P., 2016. Dissolved organic carbon reduces habitat coupling by top predators in lake ecosystems. Ecosystems 19, 955–967.
Bauer, J.E., Cai, W.-J., Raymond, P.A., Bianchi, T.S., Hopkinson, C.S., Regnier, P.A.G., 2013. The changing carbon cycle of the coastal ocean. Nature 504, 61–70.
Bianchi, T.S., Arndt, S., Austin, W.E., Benn, D.I., Bertrand, S., Cui, X., Faust, J.C., Koziorowska-Makuch, K., Moy, C.M., Savage, C., 2020. Fjords as aquatic critical zones (ACZs). Earth Sci. Rev. 203, 103145.
Blough, N.V., 2002. Chromophoric DOM in the coastal environment. Biogeochem. Mar. Dissolv. Organ. Matter 509–546.
Boyd, T.J., Osburn, C.L., 2004. Changes in CDOM fluorescence from allochthonous and autochthonous sources during tidal mixing and bacterial degradation in two coastal estuaries. Mar. Chem. 89, 189–210.
Chiou, C.T., Malcolm, R.L., Brinton, T.I., Kile, D.E., 1986. Water solubility enhancement of some organic pollutants and pesticides by dissolved humic and fulvic acids. Environ. Sci. Technol. 20, 502–508.
Colombano, D.D., Manfree, A.D., Teejay, A., Durand, J.R., Moyle, P.B., 2020. Estuarine-terrestrial habitat gradients enhance nursery function for resident and transient fishes in the San Francisco Estuary. Mar. Ecol. Prog. Ser. 637, 141–157.
Cooper, W.J., Zika, R.G., 1983. Photochemical formation of hydrogen peroxide in surface and ground waters exposed to sunlight. Science 220, 711–712.
Cory, R.M., Ward, C.P., Crump, B.C., Kling, G.W., 2014. Sunlight controls water column processing of carbon in arctic fresh waters. Science 345, 925–928.
Costanza, R., D'Arge, R., De Groot, R., Farber, S., Grasso, M., Hannon, B., Limburg, K., Naeem, S., O'Neill, R.V., Paruelo, J., Raskin, R.G., Sutton, P., Van Den Belt, M., 1997. The value of the world's ecosystem services and natural capital. Nature 387, 253–260.
Creed, I.F., Bergström, A.K., Trick, C.G., Grimm, N.B., Hessen, D.O., Karlsson, J., Kidd, K. A., Kritzberg, E., McKnight, D.M., Freeman, E.C., 2018. Global change-driven effects on dissolved organic matter composition: implications for food webs of northern lakes. Global Change Biol. 24, 3692–3714.
Danhiez, F., Vantrepotte, V., Cauvin, A., Lebourg, E., Loisel, H., 2017. Optical properties of chromophoric dissolved organic matter during a phytoplankton bloom. Implication for DOC estimates from CDOM absorption. Limnol. Oceanogr. 62, 1409–1425.
De Haan, H., De Boer, T., 1987. Applicability of light absorbance and fluorescence as measures of concentration and molecular size of dissolved organic carbon in humic Lake Tjeukemeer. Water Res. 21, 731–734.
de Wit, H.A., Stoddard, J.L., Monteith, D.T., Sample, J.E., Austnes, K., Couture, S., Fölster, J., Higgins, S.N., Houle, D., Hruška, J., 2021. Cleaner air reveals growing influence of climate on dissolved organic carbon trends in northern headwaters. Environ. Res. Lett. 16, 104009.
de Wit, H.A., Valinia, S., Weyhenmeyer, G.A., Futter, M.N., Kortelainen, P., Austnes, K., Hessen, D.O., Räike, A., Laudon, H., Vuorenmaa, J., 2016. Current browning of surface waters will be further promoted by wetter climate. Environ. Sci. Technol. Lett. 3, 430–435.
Deininger, A., Kaste, Ø., Frigstad, H., Austnes, K., 2020. Organic nitrogen steadily increasing in Norwegian rivers draining to the Skagerrak coast. Sci. Rep. 10, 1–9.
Dupont, N., Aksnes, D.L., 2013. Centennial changes in water clarity of the Baltic sea and the North sea. Estuar. Coast Shelf Sci. 131, 282–289.
Estlander, S., Nurminen, L., Olin, M., Vinni, M., Immonen, S., Rask, M., Ruuhijärvi, J., Horppila, J., Lehtonen, H., 2010. Diet shifts and food selection of perch Perca fluviatilis and roach Rutilus rutilus in humic lakes of varying water colour. J. Fish. Biol. 77, 241–256.
Evans, C.D., Monteith, D.T., Cooper, D.M., 2005. Long-term increases in surface water dissolved organic carbon: observations, possible causes and environmental impacts. Environ. Pollut. 137, 55–71.
Fabian, J., Zlatanovic, S., Mutz, M., Premke, K., 2017. Fungal–bacterial dynamics and their contribution to terrigenous carbon turnover in relation to organic matter quality. ISME J. 11, 415–425.
Finlay, J., Neff, J., Zimov, S., Davydova, A., Davydov, S., 2006. Snowmelt dominance of dissolved organic carbon in high-latitude watersheds: implications for characterization and flux of river DOC. Geophys. Res. Lett. 33.
Finstad, A.G., Andersen, T., Larsen, S., Tominaga, K., Blumentrath, S., De Wit, H.A., Tømmervik, H., Hessen, D.O., 2016. From greening to browning: catchment vegetation development and reduced S-deposition promote organic carbon load on decadal time scales in Nordic lakes. Sci. Rep. 6, 31944.
Frigstad, H., Kaste, Ø., Deininger, A., Kvalsund, K., Christensen, G., Bellerby, R.G.J., Sørensen, K., Norli, M., King, A.L., 2020. Influence of riverine input on Norwegian coastal systems. Front. Mar. Sci. 7, 332.
Hansen, A., Kraus, T., Pellerin, B., FlecD, J., Downing, B., Bergamaschi, B., 2016. Optical properties of dissolved organic matter (DOM): effects of biological and photolytic degradation. Limnol. Oceanogr. 61, 1015–1032.
Helms, J.R., Stubbins, A., Ritchie, J.D., Minor, E.C., Kieber, D.J., Mopper, K., 2008. Absorption spectral slopes and slope ratios as indicators of molecular weight, source, and photobleaching of chromophoric dissolved organic matter. Limnol. Oceanogr. 53, 955–969.
Hessen, D.O., Andersen, T., Lyche, A., 1990. Carbon metabolism in a humic lake: pool sizes and cycling through zooplankton. Limnol. Oceanogr. 35, 84–99.
Hessen, D.O., Carroll, J., Kjeldstad, B., Korosov, A.A., Pettersson, L.H., Pozdnyakov, D., Sørensen, K., 2010. Input of organic carbon as determinant of nutrient fluxes, light climate and productivity in the Ob and Yenisey estuaries. Estuar. Coast Shelf Sci. 88, 53–62.
Holmes, R.M., Coe, M.T., Fiske, G.J., Gurtovaya, T., McClelland, J.W., Shiklomanov, A.I., Spencer, R.G., Tank, S.E., Zhulidov, A.V., 2013. Climate change impacts on the hydrology and biogeochemistry of Arctic rivers. Clim. Chang. Glob. Warming Inland Waters 1–26.
Humborg, C., Danielsson, Å., Sjöberg, B., Green, M., 2003. Nutrient land–sea fluxes in oligothrophic and pristine estuaries of the Gulf of Bothnia, Baltic Sea. Estuarine. Coast. Shelf Sci. 56, 781–793.

Jaffé, R., McKnight, D., Maie, N., Cory, R., McDowell, W., Campbell, J., 2008. Spatial and temporal variations in DOM composition in ecosystems: the importance of long-term monitoring of optical properties. J. Geophys. Res.: Biogeosciences 113.
Johnson, J.B., Omland, K.S., 2004. Model selection in ecology and evolution. Trends Ecol. Evol. 19, 101–108.
Jonsson, S., Andersson, A., Nilsson, M.B., Skyllberg, U., Lundberg, E., Schaefer, J.K., Åkerblom, S., Björn, E., 2017. Terrestrial discharges mediate trophic shifts and enhance methylmercury accumulation in estuarine biota. Sci. Adv. 3, e1601239.
Kaiser, K., Canedo-Oropeza, M., McMahon, R., Amon, R.M., 2017. Origins and transformations of dissolved organic matter in large Arctic rivers. Sci. Rep. 7, 1–11.
Kartverket, 2020. Norway.
Kaste, Ø., Skarbøvik, E., Greipsland, I., Gundersen, C.B., Austnes, K., Skancke, L.B., Guerrero, J.-L., Sample, J.E., 2018. The Norwegian River Monitoring Programme–Water Quality Status and Trends 2017. NIVA-Rapport.
Koehler, B., Landelius, T., Weyhenmeyer, G.A., Machida, N., Tranvik, L.J., 2014. Sunlight-induced carbon dioxide emissions from inland waters. Global Biogeochem. Cycles 28, 696–711.
Köhler, S.J., Buffam, I., Laudon, H., Bishop, K.H., 2008. Climate's control of intra-annual and interannual variability of total organic carbon concentration and flux in two contrasting boreal landscape elements. J. Geophys. Res. 113.
Kominoski, J.S., Gaiser, E.E., Castañeda-Moya, E., Davis, S.E., Dessu, S., Julian, P., Lee, D.Y., Marazzi, L., Rivera-Monroy, V.H., Sola, A., Stingl, U., Stumpf, S., Surratt, D., Travieso, R., Troxler, T.G., 2020. Disturbance legacies increase and synchronize nutrient concentrations and bacterial productivity in coastal ecosystems. Ecology 101 (5), e02988.
Kothawala, D.N., Kellerman, A.M., Catalán, N., Tranvik, L.J., 2021. Organic matter degradation across ecosystem boundaries: the need for a unified conceptualization. Trends Ecol. Evol. 36, 113–122.
Larsen, S., Andersen, T., Hessen, D.O., 2011. Climate change predicted to cause severe increase of organic carbon in lakes. Global Change Biol. 17, 1186–1192.
Leroux, S.J., Loreau, M., 2008. Subsidy hypothesis and strength of trophic cascades across ecosystems. Ecol. Lett. 11, 1147–1156.
Lønborg, C., Carreira, C., Jickells, T., Álvarez-Salgado, X.A., 2020. Impacts of global change on ocean dissolved organic carbon (DOC) cycling. Front. Mar. Sci. 7, 466.
Massicotte, P., Asmala, E., Stedmon, C., Markager, S., 2017. Global distribution of dissolved organic matter along the aquatic continuum: across rivers, lakes and oceans. Sci. Total Environ. 609, 180–191.
McClelland, J., Townsend-Small, A., Holmes, R., Pan, F., Stieglitz, M., Khosh, M., Peterson, B., 2014. River export of nutrients and organic matter from the North slope of Alaska to the Beaufort sea. Water Resour. Res. 50, 1823–1839.
McGovern, M., Evenset, A., Borgå, K., de Wit, H.A., Braaten, H.F.V., Hessen, D.O., Schultze, S., Ruus, A., Poste, A., 2019. Implications of Coastal Darkening for Contaminant Transport, Bioavailability, and Trophic Transfer in Northern Coastal Waters. ACS Publications.
Mostofa, K.M., Sakugawa, H., 2009. Spatial and temporal variations and factors controlling the concentrations of hydrogen peroxide and organic peroxides in rivers. Environ. Chem. 6, 524–534.
Nagelkerken, I., Sheaves, M., Baker, R., Connolly, R.M., 2015. The seascape nursery: a novel spatial approach to identify and manage nurseries for coastal marine fauna. Fish Fish. 16, 362–371.
Oksanen, J., Blanchet, F., Friendly, M., Kindt, R., Legendre, P., McGlinn, D., Minchin, P., O'Hara, R., Simpson, G., Solymos, P., 2019. Package 'vegan'. R Package Version 2, pp. 5–6.
Opdal, A.F., Lindemann, C., Aksnes, D.L., 2019. Centennial decline in North Sea water clarity causes strong delay in phytoplankton bloom timing. Global Change Biol. 25, 3946–3953.
Paczkowska, J., Brugel, S., Rowe, O., Lefébure, R., Brutemark, A., Andersson, A., 2020. Response of coastal phytoplankton to high inflows of terrestrial matter. Front. Mar. Sci. 7, 80.
Parsons, T.R., 2013. A manual of chemical & biological methods for seawater analysis. Elsevier.
Pedersen, E.J., Miller, D.L., Simpson, G.L., Ross, N., 2019. Hierarchical generalized additive models in ecology: an introduction with mgcv. PeerJ 7, e6876.
Peterson, B.J., Fry, B., 1987. Stable isotopes in ecosystem studies. Annu. Rev. Ecol. Systemat. 18, 293–320.
Peuravuori, J., Pihlaja, K., 1997. Molecular size distribution and spectroscopic properties of aquatic humic substances. Anal. Chim. Acta 337, 133–149.
Pringle, C.M., 2001. Hydrologic connectivity and the management of biological reserves: a global perspective. Ecol. Appl. 11, 981–998.
R Core Team, 2019. R: A Language and Environment for Statistical Computing. R Foundation for Statistical Computing, Vienna, Austria.
Raymond, P.A., Saiers, J.E., Sobczak, W.V., 2016. Hydrological and biogeochemical controls on watershed dissolved organic matter transport: pulse-shunt concept. Ecology 97, 5–16.
Ripszam, M., Paczkowska, J., Figueira, J., Veenaas, C., Haglund, P., 2015. Dissolved organic carbon quality and sorption of organic pollutants in the Baltic sea in light of future climate change. Environ. Sci. Technol. 49, 1445–1452.
Seneviratne, S., Nicholls, N., Easterling, D., Goodess, C., Kanae, S., Kossin, J., Luo, Y., Marengo, J., McInnes, K., Rahimi, M., 2012. Changes in Climate Extremes and Their Impacts on the Natural Physical Environment.
Sholkovitz, E., Boyle, E., Price, N., 1978. The removal of dissolved humic acids and iron during estuarine mixing. Earth Planet Sci. Lett. 40, 130–136.
Sipler, R.E., Baer, S.E., Connelly, T.L., Frischer, M.E., Roberts, Q.N., Yager, P.L., Bronk, D.A., 2017. Chemical and photophysiological impact of terrestrially-derived dissolved organic matter on nitrate uptake in the coastal western Arctic. Limnol. Oceanogr. 62, 1881–1894.
Sponseller, R.A., Temnerud, J., Bishop, K., Laudon, H., 2014. Patterns and drivers of riverine nitrogen (N) across alpine, subarctic, and boreal Sweden. Biogeochemistry 120, 105–120.
Stepanauskas, R., Laudon, H., Jørgensen, N.O., 2000. High DON bioavailability in boreal streams during a spring flood. Limnol. Oceanogr. 45, 1298–1307.
Terhaar, J., Lauerwald, R., Regnier, P., Gruber, N., Bopp, L., 2021. Around one third of current Arctic Ocean primary production sustained by rivers and coastal erosion. Nat. Commun. 12, 1–10.
Thierry, S., Dick, S., George, S., Benoit, L., Cyrille, P., 2019. EMODnet Bathymetry a Compilation of Bathymetric Data in the European Waters, OCEANS 2019-Marseille. IEEE, pp. 1–7.
Thrane, J.-E., Hessen, D.O., Andersen, T., 2014. The absorption of light in lakes: negative impact of dissolved organic carbon on primary productivity. Ecosystems 17, 1040–1052.
Tjomsland, T., Kroglund, F., 2010. Modellering Av Strøm Og Saltholdighet I Sandnesfjorden Ved Risør.
Tolkkinen, M.J., Heino, J., Ahonen, S.H.K., Lehosmaa, K., Mykrä, H., 2020. Streams and riparian forests depend on each other: a review with a special focus on microbes. For. Ecol. Manag. 462, 117962.
Tranvik, L.J., Sieburth, J.M., 1989. Effects of flocculated humic matter on free and attached pelagic microorganisms. Limnol. Oceanogr. 34, 688–699.
Turner, R.E., Qureshi, N., Rabalais, N.N., Dortch, Q., Justic, D., Shaw, R.F., Cope, J., 1998. Fluctuating silicate: nitrate ratios and coastal plankton food webs. Proc. Natl. Acad. Sci. Unit. States Am. 95, 13048–13051.
Twardowski, M.S., Boss, E., Sullivan, J.M., Donaghay, P.L., 2004. Modeling the spectral shape of absorption by chromophoric dissolved organic matter. Mar. Chem. 89, 69–88.
Vähätalo, A.V., Aarnos, H., Hoikkala, L., Lignell, R., 2011. Photochemical transformation of terrestrial dissolved organic matter supports hetero-and autotrophic production in coastal waters. Mar. Ecol. Prog. Ser. 423, 1–14.
Vallières, C., Retamal, L., Ramlal, P., Osburn, C.L., Vincent, W.F., 2008. Bacterial production and microbial food web structure in a large arctic river and the coastal Arctic Ocean. J. Mar. Syst. 74, 756–773.
Vidon, P., Wagner, L.E., Soyeux, E., 2008. Changes in the character of DOC in streams during storms in two Midwestern watersheds with contrasting land uses. Biogeochemistry 88, 257–270.
Voss, M., Asmala, E., Bartl, I., Carstensen, J., Conley, D.J., Dippner, J.W., Humborg, C., Lukkari, K., Petkuviene, J., Reader, H., Stedmon, C., Vybernaite-Lubiene, I., Wannicke, N., Zilius, M., 2021. Origin and fate of dissolved organic matter in four shallow Baltic Sea estuaries. Biogeochemistry 154 (2), 385–403.
Warnes, G., Bolker, B., Bonebakker, L., Gentleman, R., Liaw, W., Lumley, T., Maechler, M., Magnusson, A., Moeller, S., Schwartz, M., Venables, B., 2019. Gplots: Various R Programming Tools for Plotting Data, R Package Version 3.0.1.1.
Wassmann, P., Svendsen, H., Keck, A., Reigstad, M., 1996. Selected aspects of the physical oceanography and particle fluxes in fjords of northern Norway. J. Mar. Syst. 8, 53–71.
Weishaar, J.L., Aiken, G.R., Bergamaschi, B.A., Fram, M.S., Fujii, R., Mopper, K., 2003. Evaluation of specific ultraviolet absorbance as an indicator of the chemical composition and reactivity of dissolved organic carbon. Environ. Sci. Technol. 37, 4702–4708.
Williams, R.L., Wakeham, S., McKinney, R., Wishner, K.F., 2014. Trophic ecology and vertical patterns of carbon and nitrogen stable isotopes in zooplankton from oxygen minimum zone regions. Deep Sea Res. Oceanogr. Res. Pap. 90, 36–47.
Wolf, R., Thrane, J.-E., Hessen, D.O., Andersen, T., 2018. Modelling ROS formation in boreal lakes from interactions between dissolved organic matter and absorbed solar photon flux. Water Res. 132, 331–339.
Wood, S.N., 2017. Generalized Additive Models: an Introduction with R. CRC press.
Xu, H., Guo, L., 2017. Molecular size-dependent abundance and composition of dissolved organic matter in river, lake and sea waters. Water Res. 117, 115–126.
Ye, F., Guo, W., Wei, G., Jia, G., 2018. The sources and transformations of dissolved organic matter in the Pearl river estuary, China, as revealed by stable isotopes. J. Geophys. Res.: Oceans 123, 6893–6908.
Ylöstalo, P., Seppälä, J., Kaitala, S., Maunula, P., Simis, S., 2016. Loadings of dissolved organic matter and nutrients from the Neva River into the Gulf of Finland–Biogeochemical composition and spatial distribution within the salinity gradient. Mar. Chem. 186, 58–71.